

Combined Use of Short-Lived Radionuclides (^{234}Th and ^{210}Po) as Tracers of Sinking Particles in the Ocean

Montserrat Roca-Martí^{1,*} and Viena Puigcorbé^{2,*}

¹Institut de Ciència i Tecnologia Ambientals (ICTA-UAB), Universitat Autònoma de Barcelona, Cerdanyola del Vallès, Spain; email: montserrat.roca.marti@uab.cat

²Department of Marine Biology and Oceanography, Institut de Ciències del Mar (ICM-CSIC), Barcelona, Spain; email: viena.puigcorbe@outlook.com

ANNUAL REVIEWS CONNECT

www.annualreviews.org

- Download figures
- Navigate cited references
- Keyword search
- Explore related articles
- Share via email or social media

Annu. Rev. Mar. Sci. 2024. 16:551–75

First published as a Review in Advance on September 14, 2023

The *Annual Review of Marine Science* is online at marine.annualreviews.org

<https://doi.org/10.1146/annurev-marine-041923-013807>

Copyright © 2024 by the author(s). This work is licensed under a Creative Commons Attribution 4.0 International License, which permits unrestricted use, distribution, and reproduction in any medium, provided the original author and source are credited. See credit lines of images or other third-party material in this article for license information.

*These authors contributed equally to this article



Keywords

radionuclides, ^{234}Th , ^{210}Po , sinking particles, biological carbon pump, particulate organic carbon export

Abstract

Radionuclides can provide key information on the temporal dimension of environmental processes, given their well-known rates of radioactive decay and production. Naturally occurring radionuclides, such as ^{234}Th and ^{210}Po , have been used as powerful particle tracers in the marine environment to study particle cycling and vertical export. Since their application to quantify the magnitude of particulate organic carbon (POC) export in the 1990s, ^{234}Th and, to a lesser extent, ^{210}Po have been widely used to characterize the magnitude of the biological carbon pump (BCP). Combining both radionuclides, with their different half-lives, biogeochemical behaviors, and input sources to the ocean, can help to better constrain POC export and capture BCP dynamics that would be missed by a single tracer. Here, we review the studies that have simultaneously used ^{234}Th and ^{210}Po as tracers of POC export, emphasizing what can be learned from their joint application, and provide recommendations and future directions.

1. INTRODUCTION

Radionuclide:

an unstable isotope that, by releasing radiation at a specific rate, decays into another isotope with a more stable nuclear configuration

Scavenging:

any process by which chemical species associate with particles and are subsequently removed from the water column

Biological carbon pump (BCP):

the suite of processes that transport organic carbon fixed by primary producers from the surface waters to the ocean's interior

The ocean contains a great variety of radionuclides that can be used as powerful tracers to study the timescales and rates of multiple marine processes, including atmosphere–ocean and land–ocean interactions, ocean circulation, sedimentation processes, and particle scavenging (Rodellas et al. 2023). The focus of this review is the use of radionuclides to quantify the vertical flux of particles in the marine environment, with particular interest in the export of particulate organic carbon (POC) associated with sinking particles. The gravitational sinking of organic particles is a key mechanism of the biological carbon pump (BCP) by which POC is transferred from the surface into the ocean's interior and sequestered at depth for long periods of time, therefore impacting Earth's carbon cycle and climate (Iversen 2023, Kwon et al. 2009, Siegel et al. 2023). This export of organic matter to the deep ocean also serves as a primary food source to subsurface biota and strongly influences the marine biogeochemical cycles of many chemical species. However, the magnitude of the BCP varies significantly across spatial and temporal scales, leading to estimates of global carbon export in the upper ocean that range from 5 to 12 Pg C y^{-1} (Nowicki et al. 2022 and references therein). Major efforts have been made to better constrain the magnitude of the BCP and develop a predictive understanding of its variability at regional and global scales, but it remains one of the most challenging and pressing research topics in marine biogeochemistry.

The naturally occurring radionuclides ^{234}Th and ^{210}Po have been extensively applied to quantify POC flux in the ocean over short timescales (Cochran & Masqué 2003, Rutgers van der Loeff & Geibert 2008, Verdeny et al. 2009), especially in recent years in the framework of large field programs (e.g., GEOTRACES; Anderson et al. 2014), providing a key opportunity to improve our understanding of ocean particle dynamics. This review aims to summarize the use of ^{234}Th and ^{210}Po as particle tracers and their combined application to constrain the export flux of POC associated with sinking particles in the ocean, as well as providing recommendations and research lines for future work.

2. ^{234}Th AND ^{210}Po AS PARTICLE TRACERS

Radionuclides used as particle tracers in the ocean generally have the following main characteristics: (a) they are particle reactive and therefore prone to associate with particles, (b) they are produced at a known rate by the decay of a parent radionuclide that is less particle reactive or is conservative in seawater (i.e., the parent radionuclide tends to remain longer than its daughter in the dissolved phase), and (c) they decay at a faster rate than their parent radionuclide. The depletion of ^{234}Th and ^{210}Po with respect to their parents (^{238}U and ^{210}Pb , respectively) in seawater was first observed in the 1960s and 1970s (e.g., Bacon et al. 1976, Bhat et al. 1969, Matsumoto 1975, Nozaki et al. 1976, Shannon et al. 1970) and used to derive residence times of ^{234}Th and ^{210}Po with respect to removal by scavenging. Since then, both radionuclides have been used extensively to study particle dynamics and the biogeochemical cycling of chemical species in the marine environment (Cochran & Masqué 2003, Rutgers van der Loeff & Geibert 2008) (Figure 1).

Applications of ^{234}Th as an ocean tracer can be grouped in four main themes: (a) vertical transport (i.e., the study of the downward flux of particles and associated chemical species in the water column), (b) particle cycling (i.e., the quantification of rates of particle transformation), (c) sediment dynamics (i.e., the study of sedimentation, sediment mixing, and resuspension), and (d) horizontal transport (i.e., the study of the lateral transport of particles and particle-reactive elements in coastal and open ocean systems) (Ceballos-Romero et al. 2022, Cochran & Masqué 2003, Lam & Marchal 2015, Rutgers van der Loeff & Geibert 2008, Waples et al. 2006). Similarly, the main applications of ^{210}Po as an ocean tracer are related to the cycling and transport of particles in the ocean (Cochran & Masqué 2003), but they also include the study of the atmosphere–ocean

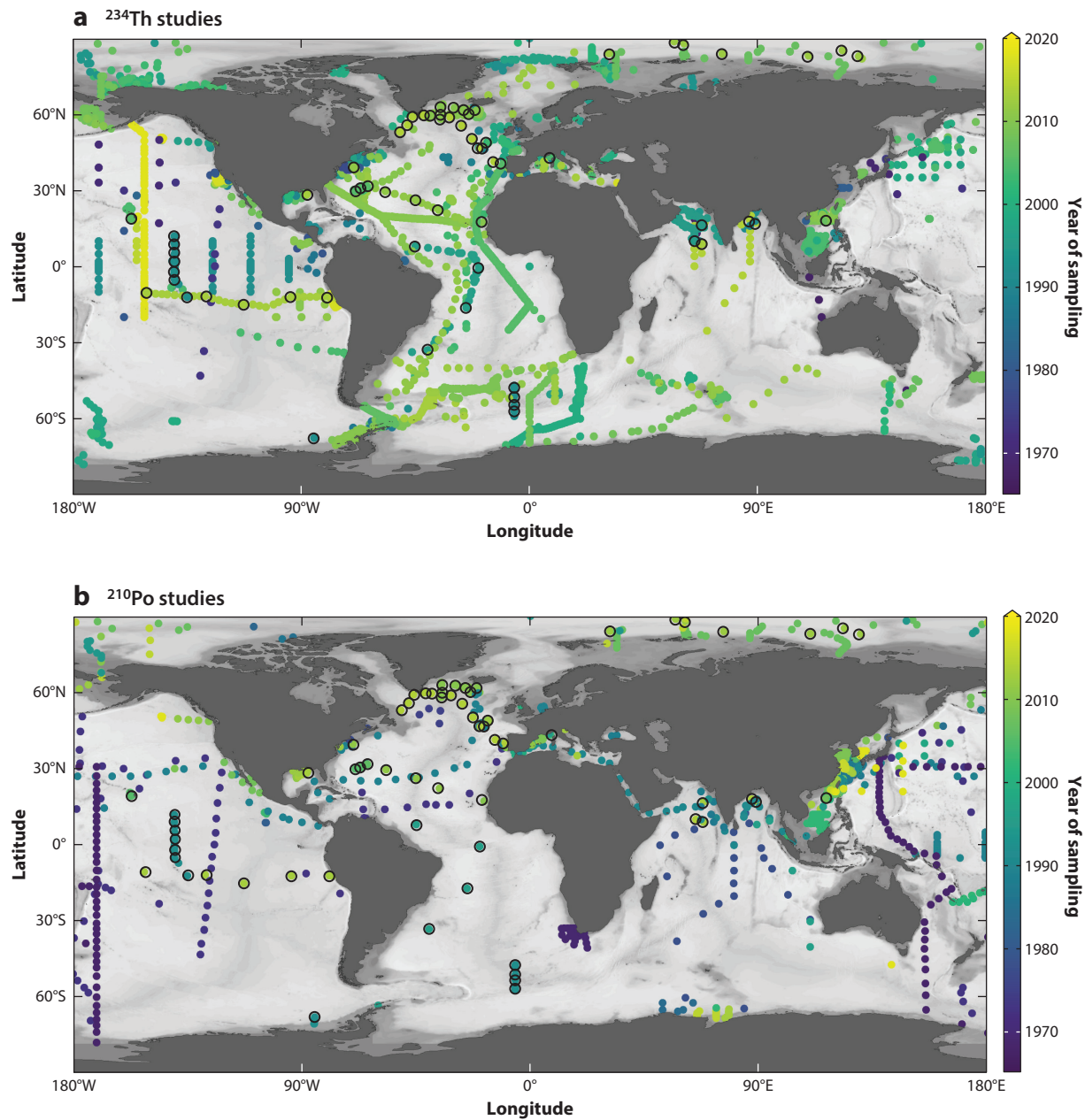


Figure 1

Compilation of sampling locations occupied for the determination of (a) ^{234}Th and (b) ^{210}Po in seawater, including seawater profiles and seawater samples from a single depth (typically from surface waters). Black-outlined circles indicate studies where both ^{234}Th and ^{210}Po were used as tracers of POC export in the open ocean (see Table 1 later in this article). Locations for ^{234}Th are from Ceballos-Romero et al. (2022), and locations for ^{210}Po are from the publications listed in the **Supplemental Material** and from unpublished data (V. Puigcorbé: GoCal4, FAMOSO, and TransArc II; M. Roca-Martí: EXPORTSNP). Abbreviation: POC, particulate organic carbon.

Supplemental Material >

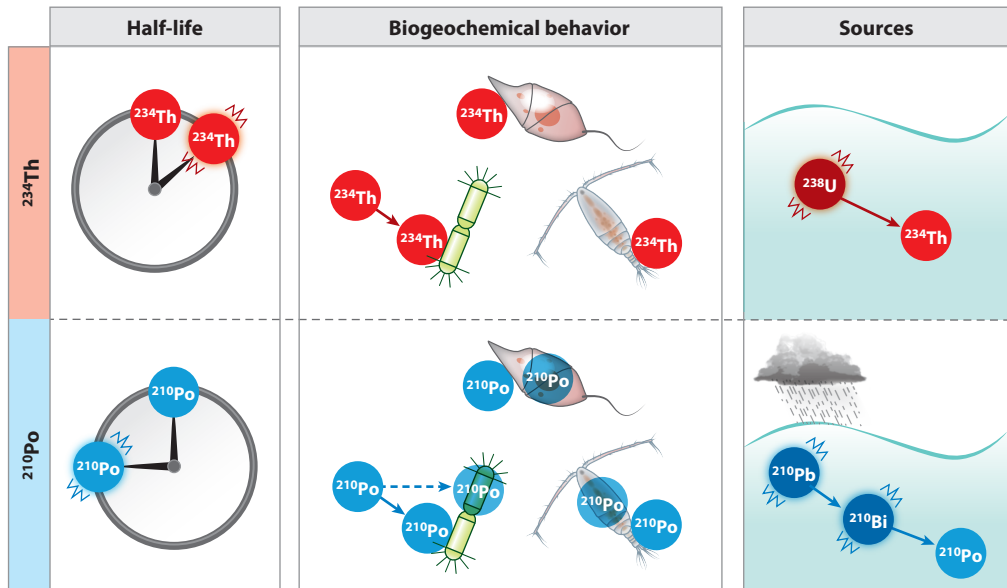


Figure 2

The main differences between ^{234}Th and ^{210}Po as particle tracers in the ocean in relation to their half-lives (shorter for ^{234}Th than for ^{210}Po), biogeochemical behaviors (surface adsorption onto particles for ^{234}Th versus surface adsorption and biological assimilation for ^{210}Po), and input sources (in situ production for ^{234}Th versus in situ production and atmospheric deposition for ^{210}Po).

interface via the quantification of, for example, the deposition velocities of aerosols (Baskaran 2011) and the study of the accumulation of ^{210}Po in marine biota, its transfer within the food chain, and its contribution to the natural radiation dose received by humans through seafood consumption (e.g., Fowler 2011, Stewart et al. 2008). Over the past few decades, both radionuclides have been widely used (^{234}Th to a larger extent) to estimate particle export fluxes of organic carbon and other chemical species of interest throughout the upper water column across a variety of spatial and temporal scales in the world's ocean (e.g., Black et al. 2019, Ceballos-Romero et al. 2022, Gustafsson et al. 1997, Hayes et al. 2018, Le Moigne et al. 2013, Tang & Stewart 2019).

Next, we present the main characteristics of ^{234}Th and ^{210}Po , highlighting what makes them great particle tracers to study the BCP (Figure 2).

2.1. Half-Life

The key difference between stable and radioactive isotopes is the fact that radionuclides decay at well-constrained rates dictated by a decay constant (λ) specific to each radionuclide. This intrinsic characteristic allows using radionuclides to capture the temporal dimension (ages and/or rates) of key environmental processes. The decay constant of a radionuclide is related to its half-life ($T_{1/2}$) as follows:

$$T_{1/2} = \frac{\ln(2)}{\lambda}. \quad 1.$$

The half-life is a crucial aspect to consider when applying radionuclides as environmental tracers, since it should fit the timescale of the process being studied. ^{234}Th decays at a faster rate than ^{210}Po ($\lambda = 0.0288 \text{ d}^{-1}$ versus 0.00501 d^{-1} , respectively), resulting in a shorter half-life of ^{234}Th compared with ^{210}Po ($T_{1/2} = 24.1 \text{ d}$ versus 138 d ; Figure 2). As a result, the time window of particle scavenging that can be tracked with ^{234}Th is shorter than that of ^{210}Po (up to 35 d versus

Half-life ($T_{1/2}$):

the time it takes to reduce the initial number of atoms of a radionuclide by 50% through radioactive decay

200 d), which is set by their decay constant and their removal by sinking particles [^{234}Th or ^{210}Po response timescale = $1/(\lambda + k)$, where k is the scavenging removal rate] (Coale & Bruland 1985, Turnewitsch et al. 2008). These timescales make both radionuclides ideal tracers of particle export in the ocean, since they can capture short (\sim days/weeks) to seasonal (\sim months) changes in primary production and the subsequent export of biogenic particles. Hence, the combined use of both radionuclides has the advantage of covering a longer time window than that captured by ^{234}Th alone and identifying possible changes in particle export over the months prior to the sampling time.

Distribution coefficient (K_d):
a coefficient that measures the partitioning of chemical species between the particulate and dissolved phases

Primordial radionuclide:
a radionuclide produced during Earth's formation approximately 4.5 billion years ago

2.2. Biogeochemical Behavior

A key characteristic of any radionuclide used as a particle tracer is its high particle affinity. However, the use of ^{234}Th and ^{210}Po as tracers of particle export is based on quantifying the disequilibrium with their parents in the upper ocean that results from their different biogeochemical behaviors. ^{234}Th is highly particle reactive, in clear contrast with ^{238}U , which has a conservative behavior in well-oxygenated seawater; both ^{210}Po and ^{210}Pb are particle reactive, but ^{210}Po is preferentially scavenged by organic particles relative to ^{210}Pb (Friedrich & Rutgers van der Loeff 2002, Verdeny et al. 2009). A way of defining the degree to which a chemical element is associated with particles is by means of its distribution coefficient (K_d) between the particulate and dissolved phases, where the higher the K_d is, the higher the particle reactivity is. For Th, Po, and Pb, K_d values in the marine environment vary on the order of 10^4 – 10^8 , 10^5 – 10^9 , and 10^3 – 10^8 L kg^{-1} , respectively, as a function of particle concentration and composition, among other factors (Bam et al. 2020, Chuang et al. 2013, Hayes et al. 2015, Tang et al. 2017).

Th is rapidly attached to particle surfaces, and its scavenging is consistent with removal by passive surface adsorption onto particles rather than active biological uptake (Honeyman et al. 1988 and references therein) (Figure 2). Several studies have shown that Th has a strong affinity to calcium carbonate and lithogenic material (e.g., Chase et al. 2002, Chuang et al. 2013, Hayes et al. 2015), and sorption experiments with colloidal organic matter have shown that Th preferentially binds to polysaccharide-enriched organic matter (Quigley et al. 2002). Regarding Po and Pb, a clear difference between them is that while Pb adsorbs only to particle surfaces (as Th does), Po is adsorbed on particles and also taken up into bacteria and phytoplankton cells following the distribution of proteins and sulfur (Cherrier et al. 1995, Fisher et al. 1983, LaRock et al. 1996, Stewart & Fisher 2003) and bioaccumulated through the food web (Fowler 2011, Stewart et al. 2008) (Figure 2). Consequently, Po is more associated with organic matter (especially proteins and sulfur-enriched compounds) than Pb is, and Pb tends to be more associated with inorganic particles, such as opal (e.g., Friedrich & Rutgers van der Loeff 2002, Stewart et al. 2007b, Tang et al. 2017). The presence of macromolecular organic compounds, such as proteins and acid polysaccharides, associated with particle surfaces and colloids could also influence the adsorption and partitioning of Po and Pb in seawater (Quigley et al. 2002; Yang et al. 2013, 2015). Overall, the fact that Po can be assimilated into cells results in a stronger association of Po with organic matter and its cycling relative to Pb and Th, which are more related to the surface area of particles (not necessarily organic).

2.3. Sources

Many of the radionuclides used as ocean tracers belong to one of the three natural decay chains. These chains start with a long-lived primordial radionuclide (^{238}U , ^{235}U , or ^{232}Th) that decays through a chain of radionuclides with shorter half-lives into a stable isotope of Pb. If not subjected to chemical or physical separation, all the radionuclides in a decay chain would reach secular

Secular equilibrium: the state when a parent and a daughter radionuclide have reached the same activity, given the much slower decay rate of the parent

Activity: the number of radioactive transformations of a radionuclide per unit of time (activity = number of atoms · decay constant)

Disintegrations per minute (dpm): a unit of activity referring to the number of decay events per minute

equilibrium. In nature, however, this equilibrium is often broken, which allows the study of the environmental processes responsible for that deviation, such as the particle transport in the ocean that causes the disequilibrium between ^{234}Th and ^{238}U or between ^{210}Po and ^{210}Pb .

^{234}Th is constantly produced in the ocean by alpha decay of ^{238}U ($T_{1/2} = 4.5 \cdot 10^9$ y; **Figure 2**), which under oxic conditions occurs almost entirely in the dissolved phase (Rutgers van der Loeff & Geibert 2008) and is closely coupled to salinity (Chen et al. 1986). Atmospheric sources of ^{238}U to the ocean are insignificant relative to its concentration in seawater. Further down in the ^{238}U decay chain, ^{210}Po is produced by beta decay of ^{210}Pb ($T_{1/2} = 22.3$ y) via a short-lived radionuclide (^{210}Bi , $T_{1/2} = 5.01$ d). Both ^{210}Po and ^{210}Pb are produced in the ocean, but they are also supplied by atmospheric deposition (**Figure 2**) from the decay of a short-lived noble gas (^{222}Rn , $T_{1/2} = 3.82$ d) and other sources (e.g., volcanic activity and fossil fuel burning; Baskaran 2011). The activities of ^{210}Pb and ^{210}Po in the atmosphere are governed largely by ^{222}Rn emanation rates from the continents (and to a much lesser extent from the oceans) and their removal during atmospheric transport by decay and scavenging by aerosols (Baskaran 2011, Church & Sarin 2008, Turekian & Graustein 2003). As a result, atmospheric inputs of ^{210}Pb and ^{210}Po to the ocean are variable, depending on, for example, the proximity to land masses, the source of air masses (continental versus oceanic), or the amount and frequency of precipitation. It is important to note that the atmospheric flux of ^{210}Po to surface waters is usually small compared with that of ^{210}Pb (typically <10–20%), given the relatively short residence times of ^{210}Pb in the atmosphere (Baskaran 2011). Therefore, in contrast to ^{234}Th , atmospheric deposition is an additional source of ^{210}Po to the upper ocean.

3. ^{234}Th AND ^{210}Po AS TRACERS OF PARTICULATE ORGANIC CARBON EXPORT

Below, we briefly describe the analytical methods used to determine ^{234}Th and ^{210}Po in seawater and the export models most applied for their use as tracers of POC export in the ocean. Information on the determination of ^{234}Th and ^{210}Po in particles can be found in papers by Church et al. (2012), Maiti et al. (2012), and Baskaran et al. (2013).

3.1. Analytical Methods in Seawater

^{234}Th and ^{210}Po in seawater are determined following radiochemistry and counting techniques that allow one to accurately quantify their low concentrations [typically ~ 2 disintegrations per minute (dpm) L^{-1} or $1.0 \cdot 10^5$ atoms L^{-1} for ^{234}Th , and ~ 0.15 dpm L^{-1} or $4.3 \cdot 10^4$ atoms L^{-1} for ^{210}Po]. The initial analytical methods were developed from the 1960s to the 1980s (Bhat et al. 1969, Fleer & Bacon 1984, Shannon & Orren 1970, Thomson & Turekian 1976). Since then, methods have improved, allowing for smaller sample volumes and more efficient protocols (Clevenger et al. 2021, Rigaud et al. 2013). Efforts to standardize protocols have also been made (Cent. Mar. Environ. Radioact. 2023), and international programs such as the Geochemical Ocean Sections Study (GEOSECS) (e.g., Chung et al. 1983) and, more recently, GEOTRACES have conducted intercalibration exercises for ^{234}Th and $^{210}\text{Po}/^{210}\text{Pb}$ (Church et al. 2012, Maiti et al. 2012).

An initial precipitation step is essential to concentrate all of these radionuclides from seawater samples. For ^{234}Th , early studies involved precipitation with Fe(OH)_3 prior to electroplating of ^{234}Th on metal disks and beta counting (Bhat et al. 1969) or the use of MnO_2 cartridges to scavenge ^{234}Th from large volumes of seawater followed by gamma counting (Bacon & Anderson 1982, Buesseler et al. 1992b). Later on, Rutgers van der Loeff & Moore (1999) developed the MnO_2 precipitation method using 20 L of seawater and subsequent filtration prior to beta counting. This method improved the separation of ^{238}U and ^{234}Th [compared with Fe(OH)_3] and allowed higher sampling resolution (compared with MnO_2 cartridges). In the early 2000s, the sampling

volume was reduced to 2–4 L (Benítez-Nelson et al. 2001, Buesseler et al. 2001), and the use of the ^{230}Th – ^{229}Th spike technique to correct for sample losses during processing was introduced (Pike et al. 2005). The quantification of ^{238}U activities is commonly inferred from salinity data (e.g., Not et al. 2012, Owens et al. 2011).

^{210}Po and ^{210}Pb are usually concentrated from seawater using the $\text{Fe}(\text{OH})_3$ (Thomson & Turekian 1976) or cobalt ammonium pyrrolidine dithiocarbamate (Co-APDC) (Fleer & Bacon 1984) precipitation techniques (Roca-Martí et al. 2021b). The analytical protocols have evolved over time, for example, regarding the sample volume (from ~20–30 L to 10 L) or the type and amount of reagents used, but they have typically involved the addition of a Po tracer (usually ^{209}Po) and stable old Pb (i.e., with low ^{210}Pb activity) to track losses during sample processing. After precipitation, the precipitate is dissolved to allow the plating of Po by spontaneous deposition onto a silver disk in diluted hydrochloric acid, while ^{210}Pb remains in solution. The disks, containing ^{210}Po and ^{209}Po , are then counted by alpha spectrometry. After >6 months, the sample is replated onto a new silver disk and measured by alpha spectrometry to determine ^{210}Pb from ^{210}Po ingrowth. Further development of the method has led to the use of anion exchange resins for Po removal after the first plating and to the determination of Pb chemical recoveries after the precipitation and ion exchange steps (Rigaud et al. 2013). Rigaud et al. (2013) provided a complete description of the calculations and uncertainties associated with decay/ingrowth, chemical recovery, and blank corrections for accurately determining ^{210}Po and ^{210}Pb in seawater.

3.2. Particulate Organic Carbon Export Models

The application of ^{234}Th and ^{210}Po as proxies for POC flux relies on measuring (a) the disequilibrium with respect to their parents throughout the upper ocean to estimate the export fluxes of ^{234}Th and ^{210}Po and (b) the POC/ ^{234}Th and POC/ ^{210}Po ratios representative of sinking particles at any depth of interest (Buesseler et al. 1992a, Cochran & Masqué 2003, Murray et al. 2005) (Figure 3). A high vertical sampling resolution is key to capture the disequilibrium

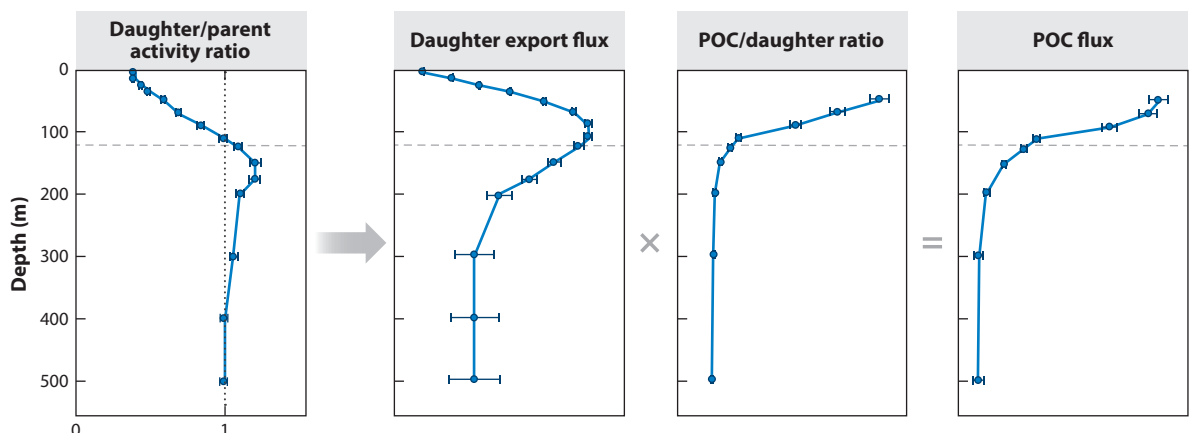


Figure 3

The steps involved in applying ^{234}Th and ^{210}Po as proxies for POC flux. First, the disequilibrium between each daughter/parent radioactive pair (^{234}Th / ^{238}U and ^{210}Po / ^{210}Pb) must be determined throughout the upper water column to calculate the export flux of the daughter radionuclide associated with sinking particles using a scavenging model. This export flux is then converted into POC flux by measuring the ratio between POC and the daughter radionuclide (POC/ ^{234}Th and POC/ ^{210}Po) on sinking particles (for details, see Section 3.2). In the first panel, the vertical dotted line shows secular equilibrium between daughter and parent radionuclide (daughter/parent activity ratio = 1). In all panels, the horizontal dashed line denotes the base of the euphotic zone. Abbreviation: POC, particulate organic carbon.

between $^{234}\text{Th}/^{238}\text{U}$ and $^{210}\text{Po}/^{210}\text{Pb}$ in the upper water column (**Figure 3**). Deficits of ^{234}Th and ^{210}Po are typically found in the upper tens or hundreds of meters of the water column due to their preferential removal by sinking particles compared with ^{238}U and ^{210}Pb , respectively (i.e., daughter/parent activity ratios < 1). In subsurface waters, excess of ^{234}Th and ^{210}Po can be found (i.e., daughter/parent activity ratios > 1), reflecting remineralization or disaggregation of particles to nonsinking phases. Secular equilibrium is found with increasing water depth where there is no net removal or addition of ^{234}Th or ^{210}Po faster than their ingrowth/decay rates (i.e., daughter/parent activity ratios = 1).

Scavenging models can have different levels of complexity based on how many types of particles are considered (Savoye et al. 2006). However, the application of ^{234}Th and ^{210}Po as proxies for POC flux generally involves the use of one-box scavenging models because determining total activities (dissolved + particulate phases together) is enough to quantify $^{234}\text{Th}/^{238}\text{U}$ and $^{210}\text{Po}/^{210}\text{Pb}$ disequilibrium in seawater. Thus, the export flux of ^{234}Th and ^{210}Po can be assessed using a general activity balance where their activities in seawater (activity of the daughter radionuclide, A_D) change with time as a function of the ingrowth from the decay of their parents ($\lambda_D A_P$), their radioactive decay ($\lambda_D A_D$), their removal onto sinking particles (F_D), transport processes that can add or remove them by advection and diffusion (V), and their input by atmospheric deposition (F_{atm} , applicable only to ^{210}Po):

$$\frac{\partial A_D}{\partial t} = \lambda_D A_P - \lambda_D A_D - F_D + V + F_{\text{atm}}. \quad 2.$$

This equation is usually simplified by considering steady-state (SS) conditions ($\partial A_D / \partial t = 0$) and disregarding physical transport ($V = 0$) and the atmospheric input of ^{210}Po ($F_{\text{atm}} = 0$). In doing so, one can calculate the SS flux of ^{234}Th or ^{210}Po ($F_{D,SS}$, dpm m $^{-2}$ d $^{-1}$) at any depth of interest (z) by integrating the deficit of the daughter radionuclide with respect to its parent, from the surface to z (dpm m $^{-2}$), multiplied by the decay constant of the daughter radionuclide (d $^{-1}$):

$$F_{D,SS} = \int_0^z \lambda_D (A_P - A_D) dz. \quad 3.$$

In most open ocean settings, the V term is assumed to be negligible in comparison with the downward flux of the daughter radionuclide driven by sinking particles. However, in areas where radionuclide activity gradients and physical transport are significant, such as in coastal or upwelling/downwelling areas or regions with highly energetic (sub)mesoscale structures, neglecting those processes could bias radionuclide flux estimates (Resplandy et al. 2012 and references therein). Determining the V term requires an appropriate sampling coverage to capture spatial gradients in radionuclide activities, as well as accurate information on the advective and diffusive components of relevance in each study, which are usually derived from models (i.e., velocities and diffusivity coefficients; Savoye et al. 2006).

The assumption of SS conditions is usually valid in oligotrophic regions year-round, but in areas with higher seasonal variability in particle export it may fail, especially when radionuclide activities change rapidly with time (Ceballos-Romero et al. 2018). To apply a non-steady-state (NSS) model, the same water masses should be resampled within a timescale shorter or comparable to the half-life of the radionuclide (e.g., 2–3 weeks for ^{234}Th ; Ceballos-Romero et al. 2018), ideally in a Lagrangian fashion to minimize the impact of physical transport (Resplandy et al. 2012, Savoye et al. 2006). Applying an NSS model following a Lagrangian time-series sampling strategy was crucial, for example, to study the effect of Fe fertilization on particle export in the Southern Ocean using ^{234}Th (e.g., Buesseler et al. 2005). Another illustrative example of the usefulness of applying an NSS model during rapidly changing conditions can be found in a North

Atlantic process study by Clevenger et al. (S.J. Clevenger, C.R. Benitez-Nelson, M. Roca-Martí, W. Bam, M. Estapa, et al., manuscript in review). In that study, the collection of a large number of ^{234}Th samples over 4 weeks at high temporal frequency allowed the capture of a strong decrease in ^{234}Th activities in the upper water column during the decline of a diatom bloom and demonstrated the inaccuracy of the SS model in such conditions. It is also important to consider that when an SS model is used, the longer integration timescale of ^{210}Po (see Section 2.1) also results in an integration of a larger spatial area. In other words, the ^{210}Po deficits observed in the upper ocean may be the result of particle export that occurred further away from the sampling site than that of ^{234}Th , and therefore the V term may be more difficult to constrain for ^{210}Po (Stewart et al. 2010).

After the radionuclide export fluxes are quantified, it is necessary to determine the $\text{POC}/^{234}\text{Th}$ and $\text{POC}/^{210}\text{Po}$ ratios on the sinking particles [$(\text{POC}/A_D)_{\text{sinking}}$, $\mu\text{mol C dpm}^{-1}$] that are responsible for the deficits of ^{234}Th or ^{210}Po in the water column. This allows the conversion of radionuclide export fluxes (F_D , $\text{dpm m}^{-2} \text{d}^{-1}$) into POC fluxes ($\text{mmol C m}^{-2} \text{d}^{-1}$) (Figure 3):

$$\text{POC flux} = F_D \cdot \frac{(\text{POC}/A_D)_{\text{sinking}}}{1,000}. \quad 4.$$

There have been two global compilations of $\text{POC}/^{234}\text{Th}$ ratios (Buesseler et al. 2006, Puigcorbé et al. 2020) that highlighted the significant regional, temporal, vertical, and methodological variability of these ratios. However, both studies reported a decrease of the ratios with depth and recommended sampling the particles below the mixed layer. For $\text{POC}/^{210}\text{Po}$ ratios, such global compilations do not exist and the data available are more limited, but these ratios also show a general decrease with depth and significant variability across observations, especially in the upper water column (Tang & Stewart 2019). Therefore, studies must use site- and depth-specific POC/radionuclide data and measure this parameter at multiple depths in the upper water column if the objective is to study how POC flux attenuates with depth (Figure 3). It is also important to determine POC flux at depths relative to the base of the euphotic zone (typically determined from light or chlorophyll fluorescence data) rather than at a fixed depth, to allow comparison between studies and facilitate regional and global assessments of BCP efficiencies and carbon budgets (Buesseler et al. 2020b).

Sampling methods to collect particles and determine POC/radionuclide ratios have varied and improved over the years (e.g., Baker et al. 2020, Bishop et al. 2012), with sediment traps and large-volume in situ pumps being the most recommended devices for this purpose; sediment traps allow the collection of sinking particles, and in situ pumps allow higher sampling resolution, size fractionation, and the collection of rare large particles that can be important contributors to export (e.g., salp fecal pellets; Durkin et al. 2021) but missed by small-volume sampling techniques (Buesseler et al. 2006). When using in situ pumps, these ratios have been historically obtained from large particles (i.e., $>50 \mu\text{m}$), although several studies have pointed out the significant role of small particles in export, particularly in oligotrophic regions (Durkin et al. 2015, Puigcorbé et al. 2015, Richardson 2019). To overcome method-specific limitations as much as possible, it is strongly recommended to obtain POC/radionuclide ratios from various sampling methods (e.g., in situ pumps and traps) to better constrain this key parameter. Overall, the conversion of radionuclide fluxes to POC fluxes fails only if a significant fraction of the sinking particles is neglected and has a different POC/radionuclide ratio than the one used in Equation 4.

Euphotic zone:

the upper layer of the ocean, where there is enough sunlight to allow the fixation of carbon dioxide into organic matter via photosynthesis

BCP efficiency:

the fraction of net primary production that is exported to a reference depth below the euphotic zone

4. COMBINED USE OF ^{234}Th AND ^{210}Po TO CONSTRAIN PARTICULATE ORGANIC CARBON FLUXES

In this section, we review the studies that have simultaneously used ^{234}Th and ^{210}Po as proxies for POC flux to illustrate what can be learned from their joint application.

A review of the combined use of ^{234}Th and ^{210}Po to estimate POC fluxes in various regions of the world's ocean was first presented by Verdeny et al. (2009) (8 studies; see **Table 1**). That review found a trend for higher POC flux estimates derived from ^{234}Th (^{234}Th -POC fluxes, up to 40 mmol C m $^{-2}$ d $^{-1}$) relative to those obtained using ^{210}Po (^{210}Po -POC fluxes, up to 20 mmol C m $^{-2}$ d $^{-1}$), which the authors attributed to their differences in half-life and biogeochemical behavior, as well as methodological aspects. To our knowledge, 11 additional studies have estimated POC fluxes using ^{234}Th and ^{210}Po in the open ocean since then, resulting in a total of 19 studies and 114 sampling stations (see black-outlined circles in **Figure 1**). The results from all the studies are summarized in **Table 1**, classified according to the method used to determine POC/radionuclide ratios: sediment traps (studies 1 and 2 in the table), large-volume in situ pumps (studies 3–12), collection bottles (studies 13 and 14), a combination of bottles and pumps (studies 15 and 16), or the POC inventory method (studies 17–19). The POC flux estimates compiled here correspond to depths ranging from 15 to 200 m. When several estimates per station were reported for both tracers, only the estimates calculated at (or as close as possible to) the base of the euphotic zone were considered. Most of the estimates were obtained using an SS model (the sole exception being study 15) and neglecting physical transport processes (with the exceptions being studies 1 and 11) and cover a wide range of oceanic regions and timescales with respect to POC flux dynamics.

Hereafter, we focus our analysis on the studies that used either sediment traps or pumps (studies 1–12, 83 stations), since these are the methods that are considered to work best to determine POC/radionuclide ratios for the conversion of radionuclide to POC fluxes (Section 3.2). At these 83 stations, ^{234}Th -POC fluxes ranged from negligible to 40 mmol C m $^{-2}$ d $^{-1}$, with an average of 6.2 ± 6.5 mmol C m $^{-2}$ d $^{-1}$, and ^{210}Po -POC fluxes varied from negligible to 30 mmol C m $^{-2}$ d $^{-1}$, with an average of 5.5 ± 5.4 mmol C m $^{-2}$ d $^{-1}$. Comparing station by station, we found that POC fluxes are within a factor of 2 at 39% of the sampling sites (see the shaded areas and dashed lines in **Figure 4**), while the rest of the stations show either higher ^{234}Th -POC fluxes (31%) or higher ^{210}Po -POC fluxes (30%) relative to the other radionuclide by more than a factor of 2. POC flux estimates within a factor of 2 are deemed to be in good agreement, considering the complexity of the BCP and the differences often found when measuring POC fluxes with multiple independent methods (Buesseler et al. 2006). Therefore, below we use this threshold to discuss the level of agreement between ^{234}Th -POC and ^{210}Po -POC flux estimates.

To understand the causes leading to the agreement or disagreement between the estimates derived from ^{234}Th and ^{210}Po and try to identify how the intrinsic characteristics of both tracers may impact the results, below we analyze the trends observed in this compilation based on their main differences: half-life, biogeochemical behavior, and input sources to the ocean (**Figure 2**). We also discuss other factors related to methodological aspects.

4.1. Half-Life and Particulate Organic Carbon Flux Dynamics

One of the most important factors to consider when interpreting radionuclide-derived POC flux estimates is their half-life (Section 2.1). In areas where POC fluxes tend to be low and have little seasonal variability, one would expect to find small differences between POC flux estimates derived from ^{234}Th and those derived from ^{210}Po despite their different half-lives. Conversely, in areas where BCP dynamics and particle export are more variable throughout the year, the different timescales of both tracers could capture changes in POC flux over time. To assess whether the compilation shows trends in ^{234}Th -POC and ^{210}Po -POC flux estimates that can be explained by their half-life and the POC flux dynamics of the study area, stations have been divided using two classifications. First, they have been grouped into oligotrophic, non-oligotrophic, and upwelling (**Figure 4a,c**). Stations affected by upwelling have a separate category since differences in POC flux estimates between both tracers in such areas may arise from biases associated with physical

Table 1 Compilation of studies using ^{234}Th and ^{210}Po as tracers of particulate organic carbon (POC) export in the open ocean

Study ID	Study area ^a	Area type ^b	Reference depth (m) ^c	Flux model ^d	POC/radionuclide ratio sampling method ^e	Number of stations for both tracers ^f	Bloom phases ^g	^{210}Po -POC fluxes (mmol C m ⁻² d ⁻¹) ^h	^{234}Th -POC fluxes (mmol C m ⁻² d ⁻¹) ^h	^{210}Po -POC/ ^{234}Th -POC flux ratio ⁱ	Reference(s) ^j
1	Central equatorial Pacific	O, N, U	120 (0.1% light level)	SS with advection correction	Traps	9	ND	1.3–13 (5.0)	2.0–4.3 (2.4)	0.3–4.8 (2.1)	Murray et al. 2005 (data from Verdely et al. 2009)
2	South China Sea: SEATS site	O	100	SS	Traps	6	ND	1.8–20 (8.2)	9.6–21 (13)	0.2–1.4 (0.5)	Wei et al. 2011
3	North Atlantic: Sargasso Sea	O	150	SS	Pumps (>53 μm)	4	B	1.5–4.5 (3.4)	0.6–1.2 (0.9)	2.5–7.5 (2.8)	Buesseler et al. 2008 (included in Verdely et al. 2009)
4	North Atlantic: Irminger and Iceland Basins	N	140–200 (MLD + 110 m)	SS	Pumps (>53 μm)	13	D	3.3–24 (12)	5.0–26 (10)	0.3–3.0 (1.2)	Céballos-Romero et al. 2016
5	North Atlantic: Porcupine Abyssal Plain	N	150	SS	Pumps (>53 μm)	9	P	1.1–5.1 (2.5)	1.7–18 (7.0)	0.2–2.8 (0.5)	Le Moigne et al. 2013
6	North Atlantic: Gulf of Mexico	O	150	SS	Pumps (>51 μm)	6	N	1.6–3.3 (1.9)	1.6–3.4 (2.5)	0.5–1.2 (0.9)	Maiti et al. 2016
7	North Atlantic: GA03 section	O, N, U	54–197 (PPZ)	SS	Pumps (1–51 μm)	6	N, B, D	1.3–9.5 (3.7)	0.1–3.2 (0.8)	0.4–26 (5.0)	Owens et al. 2015, Rigaud et al. 2015 (data from Hayes et al. 2018)
8	Central Arctic	O	15–50	SS	Pumps (>53 μm)	7	N	0.1–6.3 (1.7)	Negligible–6.7 (0.9)	0.1–5.3 (2.0)	Roca-Martí et al. 2016
9	Mediterranean Sea: DYFAMED site	N	200	SS	Pumps (>70 μm)	3	B, ND	4.4–6.7 (4.8)	4.7–18 (13)	0.3–1.0 (0.4)	Stewart et al. 2007 ^a (included in Verdely et al. 2009)

(Continued)

Table 1 (Continued)

Study ID	Study area ^a	Area type ^b	Reference depth (m) ^c	Flux model ^d	POC/radionuclide ratio sampling method ^e	Number of stations for both tracers ^f	^{210}Po -POC fluxes (mmol C m ⁻² d ⁻¹) ^h	^{210}Po -POC/ ^{234}Th -POC flux ratio ⁱ	Reference (s)		
10	North Atlantic: Sargasso Sea (BA1S site)	O	150	SS	Pumps, average of 3 different size fractions (>10 to >100 μm)	N, B	1.9–3.0 (2.5)	3.6–7.0 (3.9)	Brew et al. 2009, Stewart et al. 2010 (data from Stewart et al. 2011)		
11	South Pacific: GP16 section	O, N, U	43–179 (PZ)	SS with upwelling correction	Pumps (> 51 μm)	6	N, B, P	0.4–30 (2.3)	0.7–40 (1.4)	0.1–3.7 (1.9)	
12	North Atlantic: GA01 section	N, U	40–120 (ThEq)	SS	Pumps (> 53 μm)	11	B, D, P Negligible-11 (2.0)	1.4–12 (6.1)	0.0–4.3 (0.4)	Lemaire et al. 2018, Tang & Stewart 2019	
13	Indian Ocean: Arabian Sea and Bay of Bengal	O, N	100	SS	Bottles (> 1 μm)	7	ND	2.1–8.5 (3.8)	0.6–8.0 (1.2)	0.4–14 (2.6)	Anand et al. 2018
14	Southern Ocean: Antarctic Circumpolar Current	N	60–100	SS	Bottles (> 0.7–1 μm)	8	B, ND	4.8–17 (10)	3.9–38 (13)	0.2–3.7 (0.8)	Friedrich & Rutgers van der Loeff 2002 (data from Verdely et al. 2009)
15	North Atlantic: NABE	N	150	NSS	Bottles (> 0.4–0.7 μm) (Po), bottles and pumps (>0.5–0.7 μm) (Th)	1	D	23	45	0.5	Buesseler et al. 1992a, Horowitz et al. 2020
16	South equatorial Atlantic	N, U	100–150	SS	Bottles and pumps (>0.7 μm) (Po), pumps (>0.7 μm) (Th)	4	ND	1.4–8.5 (4.9)	1.1–3.8 (2.5)	1.3–2.2 (1.9)	Charette & Moran 1999, Sarin et al. 1999 (data from Verdely et al. 2009)

(Continued)

Table 1 (Continued)

Study ID	Study area ^a	Area type ^b	Reference depth (m) ^c	Flux model ^d	POC/radionuclide ratio sampling method ^e	Number of stations for both tracers ^f	Bloom phase ^g	^{210}Po -POC fluxes (mmol C m ⁻² d ⁻¹) ^h	^{234}Th -POC fluxes (mmol C m ⁻² d ⁻¹) ^h	^{210}Po -POC/ ^{234}Th -POC flux ratio ⁱ	Reference(s)
17	North Atlantic: Sargasso Sea (BATS site)	O	150	NA	POC inventory/ particulate radionuclide residence time	6	B, ND	2.4–8.0 (4.0)	0.3–2.5 (7.4)	0.2–9.0 (0.6)	Kim & Church 2001 (data from Verdely et al. 2009)
18	Antarctica: Bellingshausen Sea	U	100	NA	POC inventory/ particulate radionuclide residence time	1	ND	2.3	24	0.1	Shinnmöld et al. 1995 (data from Verdely et al. 2009)
19	North tropical Pacific: Hawaii	O	150	NA	POC inventory/ particulate radionuclide residence time	4	D, ND	1.6–1.7 (1.7)	0.1–1.2 (0.6)	1.4–19 (3.0)	Maiti et al. 2008, Verdely et al. 2008 (data from Verdely et al. 2009)

Data are from the cited publications. If the authors reported flux estimates using several approaches, only one is considered here, as detailed in the table. All POC flux estimates were obtained using a consistent methodology for both tracers to allow comparison.

^aOcean region studied. Abbreviations: BATS, Bermuda Atlantic Time-series Study; DYFAMED, Dynamique des Flux Atmosphériques en Méditerranée; NABE, North Atlantic Bloom Experiment; SEATS, Southeast Asia Time-series Study.

^bType of study area based on information from the studies: O, oligotrophic; N, non-oligotrophic; U, upwelling.

^cReference depth used for estimating POC flux. Only the estimates calculated at (or as close as possible to) the base of the euphotic zone were considered (one estimate per station). Abbreviations: MLD, mixed-layer depth; PPZ, primary production zone; ThEq, ^{234}Th / ^{238}U equilibrium depth.

^dDetails of the model used for calculating the export flux of ^{234}Th and ^{210}Po . Abbreviations: NA, not applicable; NSS, non-steady state; SS, steady state (see Section 3.2).

^eDetails of the sampling method used to collect particles and determine POC/ ^{234}Th and POC/ ^{210}Po ratios, and information on the particle-size class considered when using in situ pumps and collection bottles (see Section 3.2).

^fNumber of stations where both tracers were used as proxies for POC flux.

^gStations classified according to the bloom phase at the time of sampling: N, no bloom; B, bloom; D, bloom decline; P, postbloom; ND, not determined. The classification is based on information provided by the studies if available. No bloom means that there was no indication of a phytoplankton bloom occurring at the time of sampling or over the last \sim 3 months; bloom means that a bloom developed at the time of sampling (before the bloom peak); bloom decline means that a bloom was declining at the time of sampling (after the bloom peak); and postbloom means that there were indications that a bloom had occurred over the \sim 3 months prior to sampling. It is important to note that the definition of a bloom may differ between studies. When different bloom phases are reported for a single study, that indicates that not all stations were sampled at the same bloom phase.

^hRange and median (in parentheses) of the POC fluxes estimated using ^{210}Po (^{210}Po -POC fluxes) and ^{234}Th (^{234}Th -POC fluxes).

ⁱRange and median (in parentheses) of the ratio between ^{210}Po -POC fluxes and ^{234}Th -POC fluxes.

^jSources(s) for the table data. In some cases, the data were taken from a later paper or review that performed additional analysis using information in the original studies, and those are indicated according in parentheses.

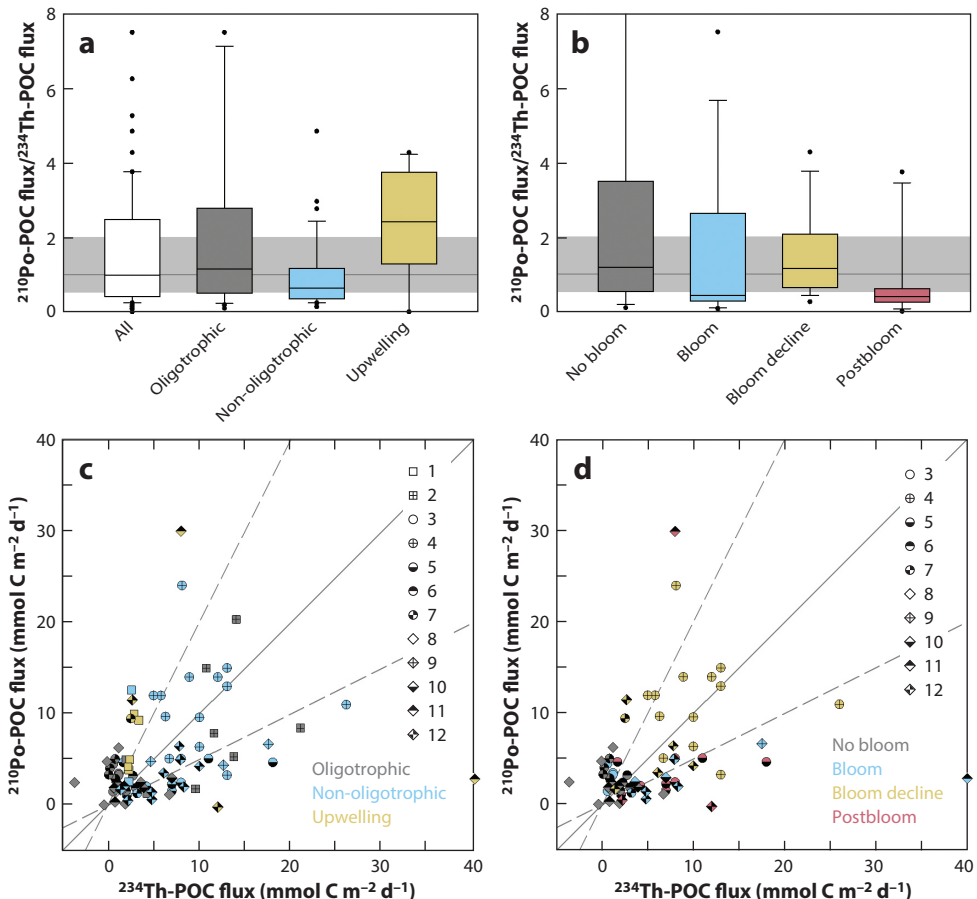


Figure 4

(a,b) Box plots of the ratio between ^{210}Po -derived POC fluxes and ^{234}Th -derived POC fluxes and (c,d) scatter plots showing the POC flux estimates obtained from each tracer at all the sampling stations from studies 1–12 (Table 1). Stations are classified as oligotrophic, non-oligotrophic, or upwelling (panels a and c) and as no bloom, bloom, bloom decline, or postbloom (panels b and d) (for details, see Table 1). The solid gray lines indicate agreement between $^{234}\text{Th-POC}$ and $^{210}\text{Po-POC}$ flux estimates, while the shaded areas (panels a and b) and dashed lines (panels c and d) indicate agreement within a factor of 2. Abbreviation: POC, particulate organic carbon.

transport. Second, stations have been classified according to the bloom stage encountered at the time of sampling: no bloom, bloom, bloom decline, and postbloom (Figure 4b,d; for definitions, see footnote g in Table 1).

Contrary to what would be expected, there is no better agreement between tracers in oligotrophic versus non-oligotrophic areas (34% versus 47% of stations show estimates within a factor of 2, respectively; Figure 4a,c), and oligotrophic stations show more spread in $^{210}\text{Po-POC}/^{234}\text{Th-POC}$ flux ratios than non-oligotrophic stations (Figure 4a). This observation suggests either that this classification is too simplistic to identify the role of the half-life in driving the trends or that other factors may be more important. On the other hand, when looking at the timing of the sampling relative to the phase of the bloom, we find better agreement between tracers in no-bloom and bloom-decline situations (41% and 58%, respectively; Figure 4b,d) than in bloom and

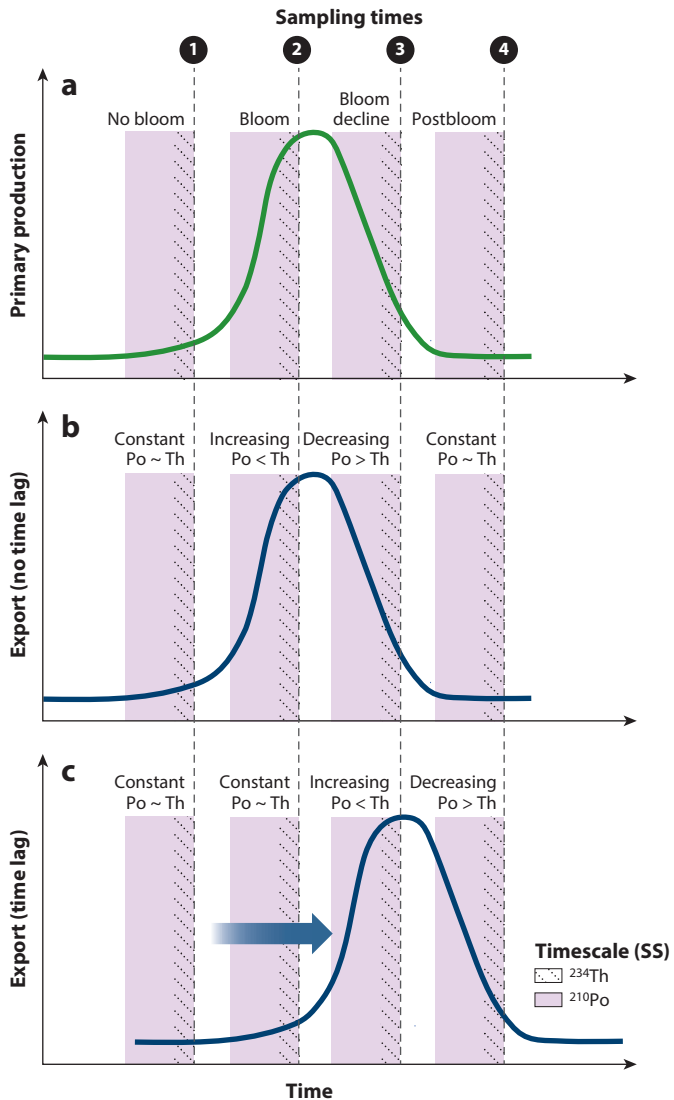


Figure 5

Integration timescales of ^{234}Th and ^{210}Po using an SS model at four hypothetical sampling times under different scenarios: different bloom phases (no bloom, bloom, bloom decline, or postbloom; panel a) and different export phases (constant, increasing, or decreasing) when there is no time lag between primary production and export (panel b) or when there is a temporal lag between primary production and export (panel c). Abbreviation: SS, steady state.

postbloom situations (15% and 25%, respectively). Below, we illustrate how the different integration timescales of ^{234}Th and ^{210}Po can explain the level of agreement found in POC flux estimates at different bloom phases, and how a time lag between primary production and export may impact the results (Figure 5).

4.1.1. No bloom. During no-bloom situations, when primary production and particle export are low and relatively constant over the integration timescales of ^{234}Th and ^{210}Po , POC fluxes

should be similar using both approaches despite the longer half-life of ^{210}Po (sampling time 1 in **Figure 5a,b**). Indeed, in the compilation we observe that no-bloom stations have a median ^{210}Po -POC/ ^{234}Th -POC flux ratio close to 1 (1.2, $n = 22$), with a large proportion of stations showing agreement between ^{234}Th -POC and ^{210}Po -POC fluxes (41%) (**Figure 4b,d**). A clear example of a study that found agreement between tracers during no-bloom conditions was conducted in the oligotrophic region of the northern Gulf of Mexico and was attributed to the SS nature of the system (study 6; Maiti et al. 2016). However, the remaining no-bloom stations of the compilation (59%) showed discrepancies between tracers that may have resulted from changes in export over time. For instance, a study conducted in the central Arctic in the late summer found lower ^{234}Th -POC flux estimates relative to ^{210}Po that were attributed to enhanced export fluxes occurring earlier in the season that were captured by ^{210}Po but missed by ^{234}Th (study 8; Roca-Martí et al. 2016).

4.1.2. Bloom. During bloom situations, when primary production increases over time in parallel to export, ^{234}Th -POC fluxes would be higher than ^{210}Po estimates given that ^{210}Po would integrate an earlier period of lower export, while ^{234}Th would capture a narrower time window of increased export (sampling time 2 in **Figure 5a,b**). However, if there was a temporal delay between production and export and export remained relatively constant over the timescales of ^{210}Po and ^{234}Th , then the POC flux estimates from both tracers would be similar (**Figure 5c**). In the compilation, we observe that bloom stations tend to have a low median ^{210}Po -POC/ ^{234}Th -POC flux ratio (0.4, $n = 13$), with a large proportion of stations showing higher ^{234}Th -POC fluxes relative to ^{210}Po (54%) and a small proportion of stations showing agreement between tracers (15%) (**Figure 4b,d**). This observation is consistent with bloom situations with no time lag or a short time lag between production and export. For example, a North Atlantic GEOTRACES study (GA01) consistently found higher ^{234}Th -POC fluxes relative to ^{210}Po at stations sampled during the development of a bloom in the western European and Iceland Basins (study 12; Lemaitre et al. 2018, Tang et al. 2019).

4.1.3. Bloom decline. During bloom-decline situations, when primary production decreases over time in parallel to export, ^{234}Th -POC fluxes would be lower than ^{210}Po estimates given that ^{234}Th would capture a narrower time window of decreased export, while ^{210}Po would integrate a period of higher export (sampling time 3 in **Figure 5a,b**). However, in the case of a time lag between production and export, export could actually increase over the integration timescales of ^{234}Th and ^{210}Po , resulting in higher ^{234}Th -POC fluxes (**Figure 5c**). In the compilation, we observe that during bloom-decline situations, the median ^{210}Po -POC/ ^{234}Th -POC flux ratio is close to 1 (1.2, $n = 19$), with a large proportion of stations showing agreement between ^{234}Th -POC and ^{210}Po -POC fluxes (58%) (**Figure 4b,d**). This suggests that export was similar over the timescales of ^{234}Th and ^{210}Po at those stations, unlike the scenarios depicted in **Figure 5**. Indeed, most of the bloom-decline stations in the compilation correspond to a North Atlantic study that occupied several locations in the Irminger and Iceland Basins during the declining phase of a long bloom that resulted in an export system relatively invariant over time (study 4; Ceballos-Romero et al. 2016).

4.1.4. Postbloom. Finally, during postbloom situations, when primary production and export are low, POC fluxes estimated using both tracers would be of similar magnitude (sampling time 4 in **Figure 5a,b**); if export from a previous bloom event was missed by ^{234}Th but captured by ^{210}Po , though, we would expect to find lower ^{234}Th -POC flux estimates (**Figure 5c**). In the compilation, however, we find a low median ^{210}Po -POC/ ^{234}Th -POC flux ratio (0.4, $n = 12$) during postbloom situations, with a large proportion of stations showing higher ^{234}Th -POC fluxes (58%)

(Figure 4b,d). This unexpected finding is driven mainly by a single study (study 5; Le Moigne et al. 2013) and was attributed to the different biogeochemical behaviors of both tracers (discussed next).

4.2. Biogeochemical Behavior and Nature of the Sinking Particles

The biogeochemical behavior of ^{234}Th and ^{210}Po can also lead to differences in POC flux estimates derived from both tracers given their different binding mechanisms (unlike ^{234}Th , ^{210}Po can be assimilated into cells) and particle affinities (Section 2.2). For example, Le Moigne et al. (2013) observed that ^{234}Th -POC fluxes were consistently higher than ^{210}Po -POC fluxes at the Porcupine Abyssal Plain (northeastern Atlantic) during postbloom conditions, contrary to expectations (Figure 5). The authors argued that ^{234}Th was more efficiently exported than ^{210}Po from the upper water column due to the sinking of lithogenic material, whereas ^{210}Po was more efficiently recycled in the upper water column (as POC) and not as affected by the export of lithogenic particles. In parallel, they also evaluated the role of using POC/radionuclide ratios measured in small (1–53 μm) and large ($>53 \mu\text{m}$) particles. For ^{234}Th -POC fluxes, using the ratios from either size class did not significantly impact the flux estimates. However, using the ratios from small particles to derive ^{210}Po -POC fluxes led to a closer agreement with ^{234}Th -POC fluxes, which, together with evidence of an important contribution of small particles to export in that study, suggested that ^{210}Po -POC fluxes could be biased by ignoring small sinking particles. Therefore, although the different biogeochemical behaviors of ^{234}Th and ^{210}Po may lead to a preferential export of either radionuclide depending on the nature of the sinking particles, the use of an appropriate POC/radionuclide ratio (Section 3.2) becomes essential to obtain accurate POC flux estimates.

4.3. Sources and Atmospheric Inputs

Another possible cause of the discrepancy between ^{234}Th -POC and ^{210}Po -POC flux estimates may be related to the atmospheric input of ^{210}Pb to the upper ocean (Section 2.3). In fact, another North Atlantic GEOTRACES study (GA03) consistently found higher ^{210}Po -POC fluxes than ^{234}Th -POC fluxes at four no-bloom stations in the oligotrophic subtropical gyre (study 7; Hayes et al. 2018, Owens et al. 2015, Rigaud et al. 2015) (Figure 6). At these stations, ^{234}Th deficits in the upper water column were small, whereas ^{210}Po deficits were found down to depths >500 m. These deficits were concurrent with large ^{210}Pb excesses relative to its parent ^{226}Ra ($^{210}\text{Pb}/^{226}\text{Ra}$ activity ratios of 2–3), indicating that a large fraction of ^{210}Pb was sourced from atmospheric deposition. Hayes et al. (2018) suggested that ^{210}Po -POC flux estimates at those stations may have been overestimated by neglecting the possible contribution of atmospheric deposition, with low $^{210}\text{Po}/^{210}\text{Pb}$ activity ratios (see Section 2.3), to the $^{210}\text{Po}/^{210}\text{Pb}$ disequilibrium found in the upper ocean.

The one-box scavenging model for ^{210}Po (Section 3.2) implicitly assumes that $^{210}\text{Po}/^{210}\text{Pb}$ disequilibrium in seawater is caused only by the preferential scavenging of ^{210}Po . However, if sampling occurs when a significant amount of atmospherically sourced ^{210}Pb has not reached secular equilibrium with ^{210}Po , then ^{210}Po deficits in seawater would reflect, to some extent, recent atmospheric inputs of ^{210}Pb rather than export and hence be too high. Therefore, as pointed out by Tang & Stewart (2019), efforts should be made to collect time-series data of ^{210}Pb atmospheric deposition and develop a technique to account for this where needed.

4.4. Methodological Aspects and Other Recommendations

As illustrated above, the joint application of ^{234}Th and ^{210}Po to quantify sinking particle fluxes is useful when either agreement or disagreement between both tracers is found. It can provide invaluable information on BCP dynamics over time, help better constrain POC export, improve

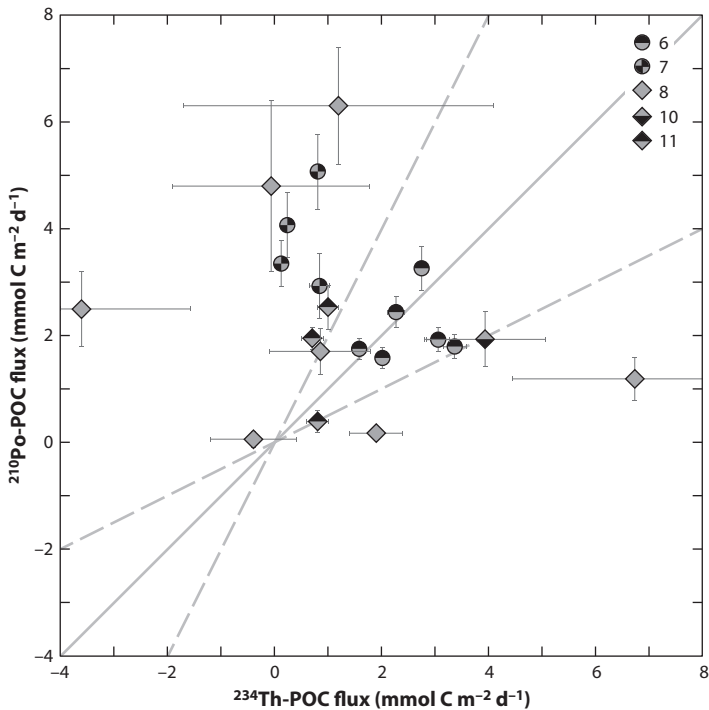


Figure 6

Scatter plot showing POC flux estimates derived from ^{234}Th and ^{210}Po at the stations classified as oligotrophic and no bloom from studies 1–12 (Table 1). The solid gray line indicates agreement between estimates derived from ^{234}Th and ^{210}Po , while the dashed lines indicate agreement within a factor of 2. Abbreviation: POC, particulate organic carbon.

the understanding of the cycling of both tracers in the ocean, or expose methodological limitations that would be unnoticed when using a single POC-flux method.

To reduce methodological biases as much as possible, it is important to pay attention to all the steps required to apply these radionuclides as proxies for particle export (Section 3). Regarding the analytical methods, a recent study comparing the two main coprecipitation techniques for scavenging ^{210}Po in duplicate seawater profiles found that a commonly used Fe(OH)_3 protocol resulted in lower activities of ^{210}Po compared with those obtained with the Co-APDC method (Roca-Martí et al. 2021b). That study concluded that ^{210}Po export fluxes, and by extension $^{210}\text{Po-POC}$ fluxes, could be overestimated when following that Fe(OH)_3 protocol, although the magnitude of the bias was found to be study-area dependent. This possible methodological bias could partly explain the large ^{210}Po deficits found in the deep ocean by multiple studies, although further research is needed to elucidate when and why Fe(OH)_3 precipitation may fail. In this compilation, ^{210}Po studies that used Fe(OH)_3 present a higher median $^{210}\text{Po-POC}/^{234}\text{Th-POC}$ flux ratio than those that used Co-APDC (1.1, $n = 94$, versus 0.5, $n = 20$, respectively), but the level of agreement between $^{234}\text{Th-POC}$ and $^{210}\text{Po-POC}$ flux estimates is similar regardless of the precipitation method. However, the limited number of ^{210}Po studies that used the Co-APDC method (only studies 8, 12, 15, and 18) and the influence of multiple factors driving differences in flux estimates between both tracers do not allow us to identify whether $^{210}\text{Po-POC}/^{234}\text{Th-POC}$ flux ratios may be biased high (and to what extent) when Fe(OH)_3 was used.

Regarding the export model, continued efforts to increase the sampling coverage for both tracers in a consistent manner (i.e., samples collected at the same time from the same depths) are crucial to characterize $^{234}\text{Th}/^{238}\text{U}$ and $^{210}\text{Po}/^{210}\text{Pb}$ disequilibrium in the water column and consider physical transport and NSS conditions when needed. Once radionuclide-derived fluxes are well constrained, the accurate quantification of POC fluxes relies on the choice of POC/radionuclide ratios. It is important to remember that there is an inherent temporal decoupling between particle collection for determining POC/radionuclide ratios and seawater collection for estimating radionuclide export fluxes—that is, the particles collected today may be different from those that generated the radionuclide disequilibrium yesterday. As an example, Roca-Martí et al. (2016) found higher ^{210}Po -derived fluxes relative to ^{234}Th -derived fluxes in the central Arctic, reflecting increased export early in the productive season. The authors suggested that the particles collected during the sampling period in the late summer were unlikely to have the same composition (and POC/ ^{210}Po ratio) as the sinking particles that created the ^{210}Po deficits in the upper water column. As a result, the lack of POC/ ^{210}Po time-series data did not allow the quantification of the POC fluxes within the ^{210}Po timescale with confidence, although the combined use of ^{234}Th and ^{210}Po in that study was key to capture particle export dynamics in the ice-covered Arctic Ocean during a time when field campaigns are rare. Therefore, collecting POC/radionuclide ratios in a time-series fashion covering the integration timescale of the tracers is strongly recommended.

FUTURE ISSUES

1. Time-series measurements of radionuclides at high spatial and temporal resolution in combination with other approaches (e.g., sediment traps and biogeochemical budgets) are needed to reduce the uncertainties associated with particulate organic carbon (POC) flux estimates and fill observational gaps. Recent efforts of major oceanographic programs are following this strategy and including radionuclides as key tools to quantify sinking particle fluxes (e.g., Buesseler et al. 2020a, Roca-Martí et al. 2021a). This will produce robust estimates of the magnitude and efficiency of the biological carbon pump (BCP) in contrasting oceanic regions that will be essential to improve ocean biogeochemical models.
2. Improvements in imaging and new sensor-based technologies allow the collection of enormous amounts of in situ data relevant to the BCP that have the potential to revolutionize this field of research. The application of radionuclides as tracers of sinking particles in a coordinated manner with emerging methods to study the BCP (e.g., Biogeochemical Argo floats; <https://biogeochemical-argo.org>) could help validate novel approaches to estimate POC export in the ocean at an unprecedented scale.
3. Measuring the sinking velocity of particles in the marine environment is not trivial, but it is an important variable controlling particle flux attenuation and the transfer of POC to the deep ocean. Sinking velocities are measured using various methods, including laboratory experiments, in situ imaging, sediment traps, marine snow catchers, and sometimes the disequilibrium of $^{210}\text{Po}/^{210}\text{Pb}$ and $^{234}\text{Th}/^{238}\text{U}$ in the water column (Villa-Alfageme et al. 2014). More extensively using these radionuclide pairs for this purpose, along with their application as tracers of particle fluxes, could be key to improving our understanding of the BCP.

4. The application of other short-lived radionuclides in combination with ^{234}Th and ^{210}Po as tracers of sinking particles could be useful to bring new insights into particle dynamics by providing valuable information on, for example, particle export deeper into the water column (^{228}Th , $T_{1/2} = 1.91$ y; Luo et al. 1995) or over very short timescales in coastal regions (^{210}Bi , $T_{1/2} = 5.01$ d; Yang et al. 2022).
5. Better understanding the biochemistry of ^{210}Po , including the formation of volatile Po species or its uptake by bacteria and transfer to higher trophic levels (Hussain et al. 1995, Kim 2001), will allow the exploration of new research avenues for using ^{210}Po as a tracer of the cycling of other chemical species in the ocean (e.g., sulfur group elements).

DISCLOSURE STATEMENT

The authors are not aware of any affiliations, memberships, funding, or financial holdings that might be perceived as affecting the objectivity of this review.

ACKNOWLEDGMENTS

We sincerely thank the Editorial Committee of the *Annual Review of Marine Science* for the opportunity to contribute to this volume. M.R.-M. acknowledges support from the Beatriu de Pinós Postdoctoral Program (2021-BP-00109) and the Ocean Frontier Institute International Postdoctoral Fellowship Program. V.P. received support from the “La Caixa” Foundation (ID 100010434) and from the European Union’s Horizon 2020 research and innovation program under Marie Skłodowska-Curie grant agreement 847648 (fellowship code LCF/BQ/PI21/11830020). This work contributes to the Institut de Ciència i Tecnologia Ambientals “María de Maeztu” Program for Units of Excellence (CEX2019-000940-M) and to the Institut de Ciències del Mar “Severo Ochoa Centre of Excellence” accreditation (CEX2019-000928-S) of the Spanish Ministry of Science and Innovation.

LITERATURE CITED

Anand SS, Rengarajan R, Shenoy D, Gauns M, Naqvi SWA. 2018. POC export fluxes in the Arabian Sea and the Bay of Bengal: a simultaneous $^{234}\text{Th}/^{238}\text{U}$ and $^{210}\text{Po}/^{210}\text{Pb}$ study. *Mar. Chem.* 198:70–87

Anderson R, Mawji E, Cutter G, Measures C, Jeandel C. 2014. GEOTRACES: changing the way we explore ocean chemistry. *Oceanography* 27(1):50–61

Bacon MP, Anderson RF. 1982. Distribution of thorium isotopes between dissolved and particulate forms in the deep sea. *J. Geophys. Res.* 87(C3):2045–56

Bacon MP, Spencer DW, Brewer PG. 1976. $^{210}\text{Pb}/^{226}\text{Ra}$ and $^{210}\text{Po}/^{210}\text{Pb}$ disequilibria in seawater and suspended particulate matter. *Earth Planet. Sci. Lett.* 32(2):277–96

Baker CA, Estapa ML, Iversen M, Lampitt R, Buesseler K. 2020. Are all sediment traps created equal? An intercomparison study of carbon export methodologies at the PAP-SO site. *Prog. Oceanogr.* 184:102317

Bam W, Maiti K, Baskaran M, Krupp K, Lam PJ, Xiang Y. 2020. Variability in ^{210}Pb and ^{210}Po partition coefficients (K_d) along the US GEOTRACES Arctic transect. *Mar. Chem.* 219:103749

Baskaran M. 2011. Po-210 and Pb-210 as atmospheric tracers and global atmospheric Pb-210 fallout: a review. *J. Environ. Radioact.* 102(5):500–13

Baskaran M, Church T, Hong G, Kumar A, Qiang M, et al. 2013. Effects of flow rates and composition of the filter, and decay/ingrowth correction factors involved with the determination of in situ particulate ^{210}Po and ^{210}Pb in seawater. *Limnol. Oceanogr. Methods* 11(3):126–38

Benitez-Nelson C, Buesseler KO, Rutgers van der Loeff M, Andrews J, Ball L, et al. 2001. Testing a new small-volume technique for determining ^{234}Th in seawater. *J. Radioanal. Nucl. Chem.* 248(3):795–99

Bhat SG, Krishnaswamy S, Lal D, Rama MWS. 1969. $^{234}\text{Th}/^{238}\text{U}$ ratios in the ocean. *Earth Planet. Sci. Lett.* 5:483–91

Bishop JKB, Lam PJ, Wood TJ. 2012. Getting good particles: accurate sampling of particles by large volume in-situ filtration. *Limnol. Oceanogr. Methods* 10:681–710

Black EE, Buesseler KO, Pike SM, Lam PJ. 2018. ^{234}Th as a tracer of particulate export and remineralization in the southeastern tropical Pacific. *Mar. Chem.* 201:35–50

Black EE, Lam PJ, Lee J-M, Buesseler KO. 2019. Insights from the ^{238}U - ^{234}Th method into the coupling of biological export and the cycling of cadmium, cobalt, and manganese in the southeast Pacific Ocean. *Glob. Biogeochem. Cycles* 33(1):15–36

Brew HS, Moran SB, Lomas MW, Burd AB. 2009. Plankton community composition, organic carbon and thorium-234 particle size distributions, and particle export in the Sargasso Sea. *J. Mar. Res.* 67(6):845–68

Buesseler KO, Andrews JE, Pike SM, Charette MA, Goldson LE, et al. 2005. Particle export during the Southern Ocean Iron Experiment (SOFeX). *Limnol. Oceanogr.* 50(1):311–27

Buesseler KO, Bacon M, Cochran JK, Livingston H. 1992a. Carbon and nitrogen export during the JGOFS North Atlantic Bloom Experiment estimated from ^{234}Th : ^{238}U disequilibria. *Deep-Sea Res. A* 39(7–8):1115–37

Buesseler KO, Benitez-Nelson CR, Moran SB, Burd A, Charette M, et al. 2006. An assessment of particulate organic carbon to thorium-234 ratios in the ocean and their impact on the application of ^{234}Th as a POC flux proxy. *Mar. Chem.* 100(3–4):213–33

Buesseler KO, Benitez-Nelson CR, Roca-Martí M, Wyatt AM, Resplandy L, et al. 2020a. High-resolution spatial and temporal measurements of particulate organic carbon flux using thorium-234 in the northeast Pacific Ocean during the EXport Processes in the Ocean from RemoTe Sensing field campaign. *Elem. Sci. Anthr.* 8(1):30

Buesseler KO, Benitez-Nelson CR, Rutgers van der Loeff M, Andrews J, Ball L, et al. 2001. An intercomparison of small-and large-volume techniques for thorium-234 in seawater. *Mar. Chem.* 74(1):15–28

Buesseler KO, Boyd PW, Black EE, Siegel DA. 2020b. Metrics that matter for assessing the ocean biological carbon pump. *PNAS* 117(18):9679–87

Buesseler KO, Cochran JK, Bacon MP, Livingston HD, Casso SA, et al. 1992b. Determination of thorium isotopes in seawater by nondestructive and radiochemical procedures. *Deep-Sea Res. A* 39(7–8):1103–14

Buesseler KO, Lamborg C, Cai P, Escoube R, Johnson R, et al. 2008. Particle fluxes associated with mesoscale eddies in the Sargasso Sea. *Deep-Sea Res. II* 55(10–13):1426–44

Ceballos-Romero E, Buesseler KO, Villa-Alfageme M. 2022. Revisiting five decades of ^{234}Th data: a comprehensive global oceanic compilation. *Earth Syst. Sci. Data* 14(6):2639–79

Ceballos-Romero E, De Soto F, Le Moigne FAC, García-Tenorio R, Villa-Alfageme M. 2018. ^{234}Th -derived particle fluxes and seasonal variability: When is the SS assumption reliable? Insights from a novel approach for carbon flux simulation. *Geophys. Res. Lett.* 45(24):13414–26

Ceballos-Romero E, Le Moigne FAC, Henson S, Marsay CM, Sanders RJ, et al. 2016. Influence of bloom dynamics on Particle Export Efficiency in the North Atlantic: a comparative study of radioanalytical techniques and sediment traps. *Mar. Chem.* 186:198–210

Cent. Mar. Environ. Radioact. 2023. Methods cookbook. *Center for Marine and Environmental Radioactivity*. <https://cmer.whoi.edu/cookbook>

Charette MA, Moran SB. 1999. Rates of particle scavenging and particulate organic carbon export estimated using ^{234}Th as a tracer in the subtropical and equatorial Atlantic Ocean. *Deep-Sea Res. II* 46(5):885–906

Chase Z, Anderson RF, Fleisher MQ, Kubik PW. 2002. The influence of particle composition and particle flux on scavenging of Th, Pa and Be in the ocean. *Earth Planet. Sci. Lett.* 204(1):215–29

Chen JH, Lawrence Edwards R, Wasserburg GJ. 1986. ^{238}U , ^{234}U and ^{232}Th in seawater. *Earth Planet. Sci. Lett.* 80:241–51

Cherrier J, Burnett WC, LaRock PA. 1995. Uptake of polonium and sulfur by bacteria. *Geomicrobiol. J.* 13(2):103–15

Chuang C-Y, Santschi PH, Ho Y-F, Conte MH, Guo L, et al. 2013. Role of biopolymers as major carrier phases of Th, Pa, Pb, Po, and Be radionuclides in settling particles from the Atlantic Ocean. *Mar. Chem.* 157:131–43

Chung Y, Finkel R, Bacon MP, Cochran JK, Krishnaswami S. 1983. Intercomparison of ^{210}Pb measurements at GEOSECS station 500 in the northeast Pacific. *Earth Planet. Sci. Lett.* 65(2):393–405

Church TM, Rigaud S, Baskaran M, Kumar A, Friedrich J, et al. 2012. Intercalibration studies of ^{210}Po and ^{210}Pb in dissolved and particulate seawater samples. *Limnol. Oceanogr. Methods* 10:776–89

Church TM, Sarin MM. 2008. U- and Th-series nuclides in the atmosphere: supply, exchange, scavenging, and applications to aquatic processes. *Radioact. Environ.* 13:11–47

Clevenger SJ, Benitez-Nelson CR, Drysdale J, Pike S, Puigcorbé V, Buesseler KO. 2021. Review of the analysis of ^{234}Th in small volume (2–4 liters) seawater samples: improvements and recommendations. *J. Radioanal. Nucl. Chem.* 329(1):1–13

Coale KH, Bruland KW. 1985. ^{234}Th : ^{238}U disequilibria within the California Current. *Limnol. Oceanogr.* 30:22–33

Cochran JK, Masqué P. 2003. Short-lived U/Th series radionuclides in the ocean: tracers for scavenging rates, export fluxes and particle dynamics. *Rev. Mineral. Geochem.* 52(1):461–92

Durkin CA, Buesseler KO, Cetinić I, Estapa ML, Kelly RP, Omand M. 2021. A visual tour of carbon export by sinking particles. *Glob. Biogeochem. Cycles* 35(10):e2021GB006985

Durkin CA, Estapa ML, Buesseler KO. 2015. Observations of carbon export by small sinking particles in the upper mesopelagic. *Mar. Chem.* 175:72–81

Fisher NS, Burns KA, Cherry RD, Heyraud M. 1983. Accumulation and cellular distribution of ^{241}Am , ^{210}Po , and ^{210}Pb in two marine algae. *Mar. Ecol. Prog. Ser.* 11:233–37

Fleer AP, Bacon MP. 1984. Determination of ^{210}Pb and ^{210}Po in seawater and marine particulate matter. *Nucl. Instrum. Methods Phys. Res.* 223(2–3):243–49

Fowler SW. 2011. ^{210}Po in the marine environment with emphasis on its behaviour within the biosphere. *J. Environ. Radioact.* 102(5):448–61

Friedrich J, Rutgers van der Loeff M. 2002. A two-tracer (^{210}Po , ^{234}Th) approach to distinguish organic carbon and biogenic silica export flux in the Antarctic Circumpolar Current. *Deep-Sea Res. I* 49(1):101–20

Gustafsson Ö, Gschwend PM, Buesseler KO. 1997. Using ^{234}Th disequilibria to estimate the vertical removal rates of polycyclic aromatic hydrocarbons from the surface ocean. *Mar. Chem.* 57(1–2):11–23

Hayes CT, Anderson RF, Fleisher MQ, Vivancos SM, Lam PJ, et al. 2015. Intensity of Th and Pa scavenging partitioned by particle chemistry in the North Atlantic Ocean. *Mar. Chem.* 170:49–60

Hayes CT, Black EE, Anderson RF, Baskaran M, Buesseler KO, et al. 2018. Flux of particulate elements in the North Atlantic Ocean constrained by multiple radionuclides. *Glob. Biogeochem. Cycles* 32(12):1738–58

Honeyman BD, Balistrieri LS, Murray JW. 1988. Oceanic trace metal scavenging: the importance of particle concentration. *Deep-Sea Res. A* 35(2):227–46

Horowitz EJ, Cochran JK, Bacon MP, Hirschberg DJ. 2020. ^{210}Po and ^{210}Pb distributions during a phytoplankton bloom in the North Atlantic: implications for POC export. *Deep-Sea Res. I* 164:103339

Hussain N, Ferdelman TG, Church TM, Luther GW. 1995. Bio-volatilization of polonium: results from laboratory analyses. *Aquat. Geochem.* 1(2):175–88

Iversen MH. 2023. Carbon export in the ocean: a biologist's perspective. *Annu. Rev. Mar. Sci.* 15:357–81

Kim G. 2001. Large deficiency of polonium in the oligotrophic ocean's interior. *Earth Planet. Sci. Lett.* 192(1):15–21

Kim G, Church TM. 2001. Seasonal biogeochemical fluxes of ^{234}Th and ^{210}Po in the upper Sargasso Sea: influence from atmospheric iron deposition. *Glob. Biogeochem. Cycles* 15(3):651–61

Kwon EY, Primeau F, Sarmiento JL. 2009. The impact of remineralization depth on the air-sea carbon balance. *Nat. Geosci.* 2:630–35

Lam PJ, Marchal O. 2015. Insights into particle cycling from thorium and particle data. *Annu. Rev. Mar. Sci.* 7:159–84

LaRock P, Hyun JH, Boutelle S, Burnett WC, Hull CD. 1996. Bacterial mobilization of polonium. *Geochim. Cosmochim. Acta* 60(22):4321–28

Le Moigne FAC, Villa-Alfageme M, Sanders RJ, Marsay C, Henson S, García-Tenorio R. 2013. Export of organic carbon and biominerals derived from ^{234}Th and ^{210}Po at the Porcupine Abyssal Plain. *Deep-Sea Res. I* 72:88–101

Lemaitre N, Planchet F, Planquette H, Dehairs F, Fonseca-Batista D, et al. 2018. High variability of particulate organic carbon export along the North Atlantic GEOTRACES section GA01 as deduced from ^{234}Th fluxes. *Biogeosciences* 15(21):6417–37

Luo S, Ku T-L, Kusakabe M, Bishop JKB, Yang Y-L. 1995. Tracing particle cycling in the upper ocean with ^{230}Th and ^{228}Th : an investigation in the equatorial Pacific along 140°W. *Deep-Sea Res. II* 42(2):805–29

Maiti K, Benitez-Nelson CR, Rii Y, Bidigare R. 2008. The influence of a mature cyclonic eddy on particle export in the lee of Hawaii. *Deep-Sea Res. II* 55(10):1445–60

Maiti K, Bosu S, D'Sa EJ, Adhikari PL, Sutor M, Longnecker K. 2016. Export fluxes in northern Gulf of Mexico – comparative evaluation of direct, indirect and satellite-based estimates. *Mar. Chem.* 184:60–77

Maiti K, Buesseler KO, Pike SM, Benitez-Nelson C, Cai P, et al. 2012. Intercalibration studies of short-lived thorium-234 in the water column and marine particles. *Limnol. Oceanogr. Methods* 10:631–44

Matsumoto E. 1975. ^{234}Th : ^{238}U radioactive disequilibrium in the surface layer of the ocean. *Geochim. Cosmochim. Acta* 39(2):205–12

Murray JW, Paul B, Dunne JP, Chapin T. 2005. ^{234}Th , ^{210}Pb , ^{210}Po and stable Pb in the central equatorial Pacific: tracers for particle cycling. *Deep-Sea Res. I* 52(11):2109–39

Not C, Brown K, Ghaleb B, Hillaire-Marcel C. 2012. Conservative behavior of uranium versus salinity in Arctic sea ice and brine. *Mar. Chem.* 130–31:33–39

Nowicki M, DeVries T, Siegel DA. 2022. Quantifying the carbon export and sequestration pathways of the ocean's biological carbon pump. *Glob. Biogeochem. Cycles* 36(3):e2021GB007083

Nozaki Y, Thomson J, Turekian KK. 1976. The distribution of ^{210}Pb and ^{210}Po in the surface waters of the Pacific Ocean. *Earth Planet. Sci. Lett.* 32(2):304–12

Owens SA, Buesseler KO, Sims KWW. 2011. Re-evaluating the ^{238}U -salinity relationship in seawater: implications for the ^{238}U - ^{234}Th disequilibrium method. *Mar. Chem.* 127:31–39

Owens SA, Pike S, Buesseler KO. 2015. Thorium-234 as a tracer of particle dynamics and upper ocean export in the Atlantic Ocean. *Deep-Sea Res. II* 116:42–59

Pike SM, Buesseler KO, Andrews J, Savoie N. 2005. Quantification of Th-234 recovery in small volume seawater samples by inductively coupled plasma-mass spectrometry. *J. Radioanal. Nucl. Chem.* 263:355–60

Puigcorbé V, Benitez-Nelson CR, Masqué P, Verdeny E, White AE, et al. 2015. Small phytoplankton drive high summertime carbon and nutrient export in the Gulf of California and Eastern Tropical North Pacific. *Glob. Biogeochem. Cycles* 29(8):1309–32

Puigcorbé V, Masqué P, Le Moigne FAC. 2020. Global database of ratios of particulate organic carbon to thorium-234 in the ocean: improving estimates of the biological carbon pump. *Earth Syst. Sci. Data* 12(2):1267–85

Quigley MS, Santschi PH, Hung CC, Guo L, Honeyman BD. 2002. Importance of acid polysaccharides for ^{234}Th complexation to marine organic matter. *Limnol. Oceanogr.* 47(2):367–77

Resplandy L, Martin AP, Le Moigne F, Martin P, Aquilina A, et al. 2012. How does dynamical spatial variability impact ^{234}Th -derived estimates of organic export? *Deep-Sea Res. I* 68:24–45

Richardson TL. 2019. Mechanisms and pathways of small-phytoplankton export from the surface ocean. *Annu. Rev. Mar. Sci.* 11:57–74

Rigaud S, Puigcorbé V, Cámara-Mor P, Casacuberta N, Roca-Martí M, et al. 2013. A methods assessment and recommendations for improving calculations and reducing uncertainties in the determination of ^{210}Po and ^{210}Pb activities in seawater. *Limnol. Oceanogr. Methods* 11:60–78

Rigaud S, Stewart G, Baskaran M, Marsan D, Church T. 2015. ^{210}Po and ^{210}Pb distribution, dissolved-particulate exchange rates, and particulate export along the North Atlantic US GEOTRACES GA03 section. *Deep-Sea Res. II* 116:60–78

Roca-Martí M, Benitez-Nelson CR, Umhau BP, Wyatt AM, Clevenger SJ, et al. 2021a. Concentrations, ratios, and sinking fluxes of major bioelements at Ocean Station Papa. *Elem. Sci. Anthr.* 9(1):166

Roca-Martí M, Puigcorbé V, Castrillejo M, Casacuberta N, García-Orellana J, et al. 2021b. Quantifying ^{210}Po / ^{210}Pb disequilibrium in seawater: a comparison of two precipitation methods with differing results. *Front. Mar. Sci.* 8:684484

Roca-Martí M, Puigcorbé V, Rutgers van der Loeff MM, Katilein C, Fernández-Méndez M, et al. 2016. Carbon export fluxes and export efficiency in the central Arctic during the record sea-ice minimum in 2012: a joint $^{234}\text{Th}/^{238}\text{U}$ and $^{210}\text{Po}/^{210}\text{Pb}$ study. *J. Geophys. Res. Oceans* 121(7):5030–49

Rodellas V, Roca-Martí M, Puigcorbé V, Castrillejo M, Casacuberta N. 2023. Radionuclides as ocean tracers. In *Marine Analytical Chemistry*, ed. J Blasco, A Tovar-Sánchez, pp. 199–273. Cham, Switz.: Springer

Rutgers van der Loeff MM, Geibert W. 2008. U- and Th-series nuclides as tracers of particle dynamics, scavenging and biogeochemical cycles in the oceans. In *U-Th Series Nuclides in Aquatic Systems*, ed. S Krishnaswami, JK Cochran, pp. 227–68. Amsterdam: Elsevier

Rutgers van der Loeff MM, Moore WS. 1999. Determination of natural radioactive tracers. In *Methods of Seawater Analysis*, ed. K Grasshoff, K Kremling, M Erhardt, pp. 365–97. Weinheim, Ger.: Verlag Chemie

Sarin MM, Kim G, Church TM. 1999. ^{210}Po and ^{210}Pb in the south-equatorial Atlantic: distribution and disequilibrium in the upper 500 m. *Deep-Sea Res. II* 46(5):907–17

Savoye N, Benítez-Nelson C, Burd AB, Cochran JK, Charette M, et al. 2006. ^{234}Th sorption and export models in the water column: a review. *Mar. Chem.* 100(3–4):234–49

Shannon LV, Cherry RD, Orren MJ. 1970. Polonium-210 and lead-210 in the marine environment. *Geochim. Cosmochim. Acta* 34(6):701–11

Shannon LV, Orren MJ. 1970. A rapid method for the determination of polonium-210 and lead-210 in sea water. *Anal. Chim. Acta* 52(1):166–69

Shimmield GB, Ritchie GD, Fileman TW. 1995. The impact of marginal ice zone processes on the distribution of ^{210}Pb , ^{210}Po and ^{234}Th and implications for new production in the Bellingshausen Sea, Antarctica. *Deep-Sea Res. II* 42(4–5):1313–35

Siegel DA, DeVries T, Cetinić I, Bisson KM. 2023. Quantifying the ocean's biological pump and its carbon cycle impacts on global scales. *Annu. Rev. Mar. Sci.* 15:329–56

Stewart G, Cochran JK, Miquel JC, Masqué P, Szlosek J, et al. 2007a. Comparing POC export from $^{234}\text{Th}/^{238}\text{U}$ and $^{210}\text{Po}/^{210}\text{Pb}$ disequilibria with estimates from sediment traps in the northwest Mediterranean. *Deep-Sea Res. I* 54(9):1549–70

Stewart G, Cochran JK, Xue J, Lee C, Wakeham SG, et al. 2007b. Exploring the connection between ^{210}Po and organic matter in the northwestern Mediterranean. *Deep-Sea Res. I* 54(3):415–27

Stewart G, Moran SB, Lomas MW, Kelly RP. 2011. Direct comparison of ^{210}Po , ^{234}Th and POC particle-size distributions and export fluxes at the Bermuda Atlantic Time-series Study (BATS) site. *J. Environ. Radioact.* 102(5):479–89

Stewart GM, Fisher NS. 2003. Experimental studies on the accumulation of polonium-210 by marine phytoplankton. *Limnol. Oceanogr.* 48(3):1193–201

Stewart GM, Fowler SW, Fisher NS. 2008. The bioaccumulation of U-and Th-series radionuclides in marine organisms. *Radioact. Environ.* 13:269–305

Stewart GM, Moran BS, Lomas MW. 2010. Seasonal POC fluxes at BATS estimated from ^{210}Po deficits. *Deep-Sea Res. I* 57(1):113–24

Tang Y, Lemaitre N, Castrillejo M, Roca-Martí M, Masqué P, Stewart G. 2019. The export flux of particulate organic carbon derived from $^{210}\text{Po}/^{210}\text{Pb}$ disequilibria along the North Atlantic GEOTRACES GA01 transect: GEOVIDE cruise. *Biogeosciences* 16(2):309–27

Tang Y, Stewart G. 2019. The $^{210}\text{Po}/^{210}\text{Pb}$ method to calculate particle export: lessons learned from the results of three GEOTRACES transects. *Mar. Chem.* 217:103692

Tang Y, Stewart G, Lam PJ, Rigaud S, Church T. 2017. The influence of particle concentration and composition on the fractionation of ^{210}Po and ^{210}Pb along the North Atlantic GEOTRACES transect GA03. *Deep-Sea Res. I* 128:42–54

Thomson J, Turekian KK. 1976. Polonium-210 and lead-210 distributions in ocean water profiles from the eastern South Pacific. *Earth Planet. Sci. Lett.* 32:297–303

Turekian KK, Graustein WC. 2003. Natural radionuclides in the atmosphere. In *Treatise on Geochemistry*, Vol. 4: *The Atmosphere*, ed. HD Holland, KK Turekian, pp. 261–79. Oxford, UK: Pergamon

Turnewitsch R, Reyss J-L, Nycander J, Waniek JJ, Lampitt RS. 2008. Internal tides and sediment dynamics in the deep sea—evidence from radioactive $^{234}\text{Th}/^{238}\text{U}$ disequilibria. *Deep-Sea Res. I* 55(12):1727–47

Verdeny E, Masqué P, Garcia-Orellana J, Hanfland C, Cochran JK, Stewart GM. 2009. POC export from ocean surface waters by means of $^{234}\text{Th}/^{238}\text{U}$ and $^{210}\text{Po}/^{210}\text{Pb}$ disequilibria: a review of the use of two radiotracer pairs. *Deep-Sea Res. II* 56(18):1502–18

Verdeny E, Masqué P, Maiti K, Garcia-Orellana J, Bruach JM, et al. 2008. Particle export within cyclonic Hawaiian lee eddies derived from ^{210}Pb - ^{210}Po disequilibrium. *Deep-Sea Res. II* 55(10–13):1461–72

Villa-Alfageme M, de Soto F, Le Moigne FAC, Giering SLC, Sanders R, García-Tenorio R. 2014. Observations and modeling of slow-sinking particles in the twilight zone. *Glob. Biogeochem. Cycles* 28(11):2014GB004981

Waples JT, Benitez-Nelson C, Savoye N, Rutgers van der Loeff M, Baskaran M, Gustafsson Ö. 2006. An introduction to the application and future use of ^{234}Th in aquatic systems. *Mar. Chem.* 100(3–4):166–89

Wei CL, Lin SY, Sheu DDD, Chou WC, Yi MC, et al. 2011. Particle-reactive radionuclides (^{234}Th , ^{210}Pb , ^{210}Po) as tracers for the estimation of export production in the South China Sea. *Biogeosciences* 8(12):3793–3808

Yang W, Guo L, Chuang C-Y, Santschi PH, Schumann D, Ayranov M. 2015. Influence of organic matter on the adsorption of ^{210}Pb , ^{210}Po and ^{7}Be and their fractionation on nanoparticles in seawater. *Earth Planet. Sci. Lett.* 423:193–201

Yang W, Guo L, Chuang C-Y, Schumann D, Ayranov M, Santschi PH. 2013. Adsorption characteristics of ^{210}Pb , ^{210}Po and ^{7}Be onto micro-particle surfaces and the effects of macromolecular organic compounds. *Geochim. Cosmochim. Acta* 107:47–64

Yang W, Tian J, Chen M, Zheng M, Chen M. 2022. A new radiotracer for particulate carbon dynamics: examination of ^{210}Bi - ^{210}Pb in seawater. *Geochim. Geophys. Geosyst.* 23(12):e2022GC010656

Contents



Annual Review of
Marine Science

Volume 16, 2024

A Life Outside <i>M.A.R. Koehl</i>	1
The Physical Oceanography of Ice-Covered Moons <i>Krista M. Soderlund, Marc Rovira-Navarro, Michael Le Bars, Britney E. Schmidt, and Theo Gerkeema</i>	25
Marine Transgression in Modern Times <i>Christopher J. Hein and Matthew L. Kirwan</i>	55
Hidden Threat: The Influence of Sea-Level Rise on Coastal Groundwater and the Convergence of Impacts on Municipal Infrastructure <i>Shellie Habel, Charles H. Fletcher, Matthew M. Barbee, and Kyrstin L. Fornace</i>	81
The Global Turbidity Current Pump and Its Implications for Organic Carbon Cycling <i>Peter J. Talling, Sophie Hage, Megan L. Baker, Thomas S. Bianchi, Robert G. Hilton, and Katherine L. Maier</i>	105
Modeling the Vertical Flux of Organic Carbon in the Global Ocean <i>Adrian B. Burd</i>	135
The Four-Dimensional Carbon Cycle of the Southern Ocean <i>Alison R. Gray</i>	163
The Impact of Fine-Scale Currents on Biogeochemical Cycles in a Changing Ocean <i>Marina Lévy, Damien Couespel, Clément Haëck, M.G. Keerthi, Inès Mangolte, and Channing J. Prend</i>	191
Climate, Oxygen, and the Future of Marine Biodiversity <i>Curtis Deutsch, Justin L. Penn, and Noelle Lucey</i>	217
Impacts of Climate Change on Marine Foundation Species <i>Thomas Wernberg, Mads S. Thomsen, Julia K. Baum, Melanie J. Bishop, John F. Bruno, Melinda A. Coleman, Karen Filbee-Dexter, Karine Gagnon, Qiang He, Daniel Murdiyarso, Kerrylee Rogers, Brian R. Silliman, Dan A. Smale, Samuel Starko, and Mathew A. Vanderklift</i>	247
Neutral Theory and Plankton Biodiversity <i>Michael J. Behrenfeld and Kelsey M. Bisson</i>	283

Using the Fossil Record to Understand Extinction Risk and Inform Marine Conservation in a Changing World <i>Seth Finnegan, Paul G. Harnik, Rowan Lockwood, Heike K. Lotze, Loren McClenachan, and Sara S. Kahanamoku</i>	307
The Microbial Ecology of Estuarine Ecosystems <i>Byron C. Crump and Jennifer L. Bowen</i>	335
Predation in a Microbial World: Mechanisms and Trade-Offs of Flagellate Foraging <i>Thomas Kiørboe</i>	361
Life in the Midwater: The Ecology of Deep Pelagic Animals <i>Steven H.D. Haddock and C. Anela Choy</i>	383
<i>Phaeocystis</i> : A Global Enigma <i>Walker O. Smith Jr. and Scarlett Trimborn</i>	417
The Evolution, Assembly, and Dynamics of Marine Holobionts <i>Raúl A. González-Pech, Vivian Y. Li, Vanessa García, Elizabeth Boville, Marta Mammone, Hiroaki Kitano, Kim B. Ritchie, and Mónica Medina</i>	443
Viruses in Marine Invertebrate Holobionts: Complex Interactions Between Phages and Bacterial Symbionts <i>Kun Zhou, Ting Zhang, Xiao-Wei Chen, Ying Xu, Rui Zhang, and Pei-Yuan Qian</i>	467
Microbialite Accretion and Growth: Lessons from Shark Bay and the Bahamas <i>R. Pamela Reid, Erica P. Suosaari, Amanda M. Oehlert, Clément G.L. Pollier, and Christophe Dupraz</i>	487
Designing More Informative Multiple-Driver Experiments <i>Mridul K. Thomas and Ravi Ranjan</i>	513
Welcoming More Participation in Open Data Science for the Oceans <i>Alexa L. Fredston and Julia S. Stewart Lowndes</i>	537
Combined Use of Short-Lived Radionuclides (^{234}Th and ^{210}Po) as Tracers of Sinking Particles in the Ocean <i>Montserrat Roca-Martí and Viena Puigcorbé</i>	551
Metal Organic Complexation in Seawater: Historical Background and Future Directions <i>James W. Moffett and Rene M. Boiteau</i>	577

Errata

An online log of corrections to *Annual Review of Marine Science* articles may be found at
<http://www.annualreviews.org/errata/marine>